Journal of Physics: Conference Series

Effect of wind directionality on fatigue life of monopile support structures for offshore wind turbines

Effect of wind directionality on fatigue life of monopile support structures for offshore wind turbines

A Nozari[1], D Kuchma[2], and E M Hines[3]

[1] Postdoctoral Scholar, Department of Civil and Environmental Engineering, Tufts University, Medford, MA, USA

[2] Professor, Department of Civil and Environmental Engineering, Tufts University, Medford, MA, USA

[3] Professor of the Practice, Department of Civil and Environmental Engineering, Tufts University, Medford, MA, USA

amin.nozari@tufts.edu

Abstract. The U.S. offshore wind industry can expect higher costs due to the lack of domestic experience with offshore wind technology. A key factor of the capital expenditure related to offshore wind farms is the cost of the support structures of offshore wind turbines. Therefore, improvements to the reliability of support structures under ultimate and fatigue loading conditions will help reduce the levelized cost of energy of offshore wind. This study presents a framework that accounts for the wind directionality by assuming a distinct and independent wind speed distribution per each wind direction and investigates its effect on the fatigue life of offshore wind turbine support structures. A monopile support structure in a potential wind site close to a National Oceanic and Atmospheric Administration buoy in the north-eastern US waters is used in this study. Fatigue damage assessment is performed for the normal operational condition of wind turbine, and the results are presented considering both cathodic protection and free corrosion conditions at the mudline level of the monopile. The location and extent of the predicted fatigue damages are found to vary due to accounting for the wind directionality.

1. Introduction

The need for renewable energy and the decrease in the Levelized Cost of Energy (LCOE) of offshore wind has increased the global volume of installed and planned Offshore Wind Turbines (OWTs) over the past two decades [1, 2]. The U.S. offshore wind sector, however, expects higher costs due to the lack of domestic experience with offshore wind technology [3, 4]. The Balance of System (BOS) activities are the main cost drivers for a planned wind farm, and the cost of support structures are recognized as the dominant portion of the BOS Capital Expenditure (CapEx). Therefore, improvements to the performance of support structures under ultimate loading conditions as well as improvements to support structures reliability under fatigue loadings will help reduce the LCoE of offshore wind.

According to the International Electrotechnical Commission standard IEC 61400-3 [5], the directionality of the wind as well as the directionality of the induced waves have a significant impact on the loads acting on OWT support structures. Therefore, applying a uni-directional or a multi-directional assumption for the inflow winds and waves has an influence on the estimated fatigue life of support structures. In normal operation design situation for OWTs, the uni-directional assumption is

recommended by the IEC standard for the ultimate limit state design (i.e., DLCs 1.1, 1.3, 1.4, 1.5, 1.6a, and 1.6b) to account for the worst-case scenario; however, the multi-directional wind and wave must be taken into account for the fatigue limit state design (i.e., DLC 1.2). Addressing the uncertainties associated with accounting for multi-directional wind can provide a more accurate fatigue life estimation for the support structures of offshore wind turbines.

This study accounts for a distinct and independent wind speed distribution for each wind direction to investigate the effect of wind directionality on the fatigue life of OWT support structures. The basic idea is that the distribution of wind speed varies in different directions since the strongest winds are observed in dominant wind directions at most sites. Therefore, the results of fatigue damage assessment of support structures could vary if a distinct wind speed distribution is estimated for each wind direction when multi-directional wind flow should be considered in the load case. This study focuses on a monopile support structure for the following two reasons: (i) approximately 80% of offshore wind turbines have been installed on the monopile support structures; and (ii) the process of estimating fatigue life is relatively simple for the monopiles due to their axisymmetric properties.

Section 2 presents the primary environmental conditions and estimated metocean parameters for the case study wind site. The detail of the employed reference wind turbine and time domain simulations are provided in Section 3, and the procedure of the fatigue damage assessment is described in Section 4. The results of the analyses are discussed in Section 5, and conclusions and suggestions for future work are explained in Section 6.

2. Metocean conditions

A potential wind site in the northeastern US waters, close to the National Oceanic and Atmospheric Administration (NOAA) buoy 44008 as shown in Figure 1, was considered to obtain more accurate and precise information about the environmental conditions. The metocean data from 1982 to 2018 (except year 2014) were recorded by this buoy as 1-hour mean values for SE Nantucket site. After cleaning and processing the data, a total of 237,148 data points is used to estimate the metocean parameters.

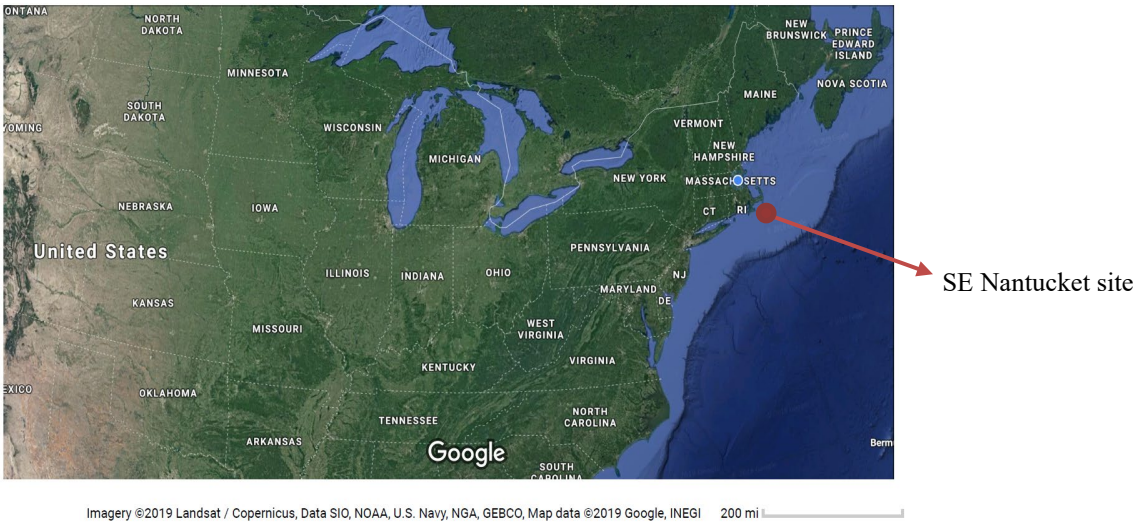

Figure 1. Location of NOAA station 44008 at southeast of Nantucket, Massachusetts, USA

2.1. Wind data

The buoy at SE Nantucket located at 4 meters above the mean sea level (MSL). A power law profile was employed to represent the wind shear and to estimate the wind velocity at hub height which is 90 meters above MSL in this study. The power law wind shear profile is defined by the following equation:

$$\bar{V}(z) = \bar{V}_r \left(\frac{z}{z_r}\right)^{\alpha} \quad (1)$$

where $\overline{V_r}$ represents the measured mean wind speed at the buoy height (z_r) and α is the roughness coefficient which is equal to 0.14 for offshore wind sites according to [5]. A Weibull probability distribution function (PDF) was fitted to the wind speed data. Eight independent Weibull distributions were subsequently fitted to the wind speed data for the main eight wind flow directions (i.e., North, Northeast, East, Southeast, South, Southwest, West, and Northwest directions). The histogram of the wind data in all directions and the fitted Weibull distributions are illustrated in Figure 2. The probability of occurrence of the wind in each direction as well as the parameters of fitted Weibull distributions for the wind speed data are presented in Table 1.

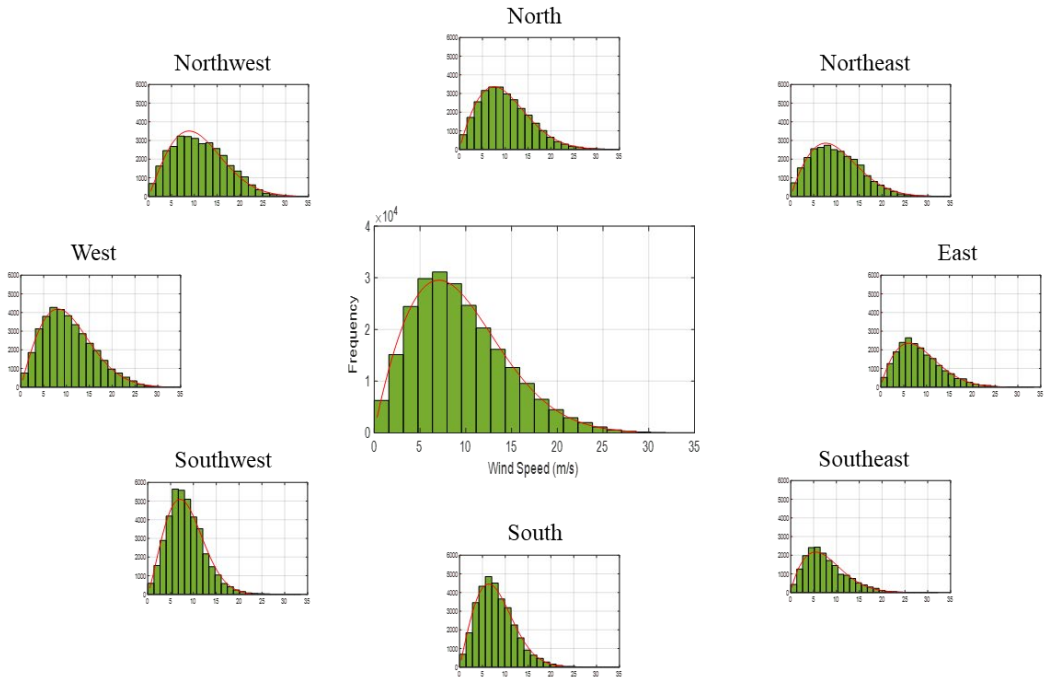

Figure 2. Average wind speed distribution and distinct wind speed distributions in eight directions adjusted to 90 meters above MSL at SE Nantucket station

The mean wind speed in Figure 2 and Table 1 is based on the recorded 1-hour mean values adjusted to the hub height (90 m above MSL). Therefore, the values given in y-axis on the histograms are the total number of hours which each wind speed bin was observed in the corresponding direction.

Table 1. Statistical characteristics of wind speed in eight directions adjusted to 90 meters above MSL

Wind direction	Probability of occurrence	Weibull distribution		
		Scale parameter	Shape parameter	Mean wind speed (m/s)
North	0.122	12.00	1.88	10.66
Northwest	0.139	13.34	1.99	11.85
West	0.155	12.50	1.95	11.09
Southwest	0.167	10.02	2.16	8.88
South	0.139	9.55	2.01	8.47
Southeast	0.077	9.20	1.78	8.17
East	0.088	10.16	1.81	9.03
Northeast	0.113	12.03	1.90	10.69
Total data	1.00	11.22	1.88	9.96

2.2. Wave parameters

According to the IEC 61400-3 standard, significant wave height, H_s, and wave peak spectral period, T_p, are the two main wave parameters which need to be estimated in order to perform a fatigue limit state design of OWT support structures. These two parameters are included in the measured data set at SE Nantucket station. Stewart et al., from the National Renewable Energy Laboratory (NREL), have developed three generic categories of metocean data for the US East Coast, West Coast, and Gulf of Mexico [7]. In order to estimate the metocean parameters, they examined a comprehensive data set from 23 offshore sites across the US where the recorded buoy data from NOAA is available. In this study, the significant wave height and wave peak spectral period were directly estimated from the SE Nantucket data set as a function of mean wind speed. The whole available data (i.e., from 36 years of measurements) were used to estimate to wave parameters. In Figure 3, the estimated wave parameters are presented for different wind speeds and compared to the proposed quantities by the NREL study for the US East Coast. It should be noted that the estimated wave height and wave peak spectral period do not change for different directions as this study tries to merely focus on the effect of wind directionality.

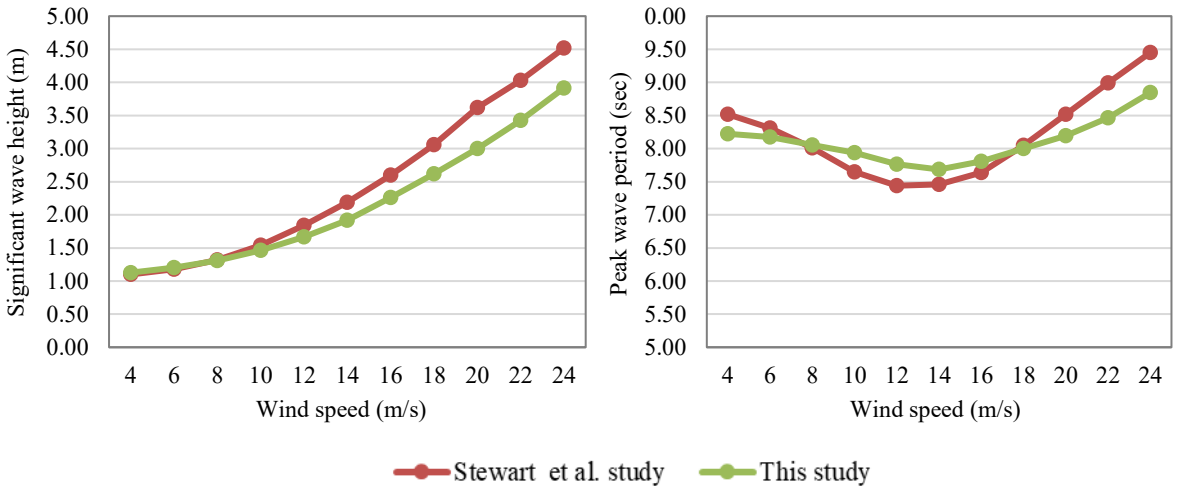

(a) Significant wave height (b) Wave peak spectral period

Figure 3. Estimated metocean parameters for different wind speed bins for SE Nantucket site and comparison with NREL estimated parameters for the US East Coast

The Pierson-Moskowitz spectrum was employed to generate the irregular wave kinematics based on the IEC standard recommendations for fatigue analysis of offshore wind turbines. The second-order wave spreading effect was included in the simulations while the breaking waves effect was not considered in this study. Different random representations were used to generate the irregular wave signals corresponding to the different mean wind speeds.

2.3. Further assumptions

Certain environmental conditions and metocean parameters cannot be estimated due to the lack of data for the case study site. For instance, sub-surface current, marine growth, and sea icing effects were not considered in this study. Seabed degradation effects, such as scour and seabed movement, and soil-structure interaction were also not investigated due to a lack of data; however, their impact on the fatigue life of offshore support structures could be significant [8].

3. Wind turbine simulations

3.1. Refence wind turbine

This study used the NREL 5 MW reference wind turbine on a monopile support structure with geometry configurations and material properties as defined in the Offshore Code Comparison Collaboration (OC3)

project for the International Energy Agency (IEA) [9, 10]. The main properties of the NREL 5 MW wind turbine on the OC3 monopile are summarized in Table 2. The hub height for this OWT is 90 meters above the MSL, and the RNA (Rotor-Nacelle Assembly) is supported by a 77.6 m linearly tapered tubular steel tower. The monopile was also designed as a tubular steel pile with 30 m length and constant section properties as provided in Table 2. Twenty meters of the monopile is embedded in the water from a presumed rigid foundation at the seabed up to the sea surface, and the remaining ten meters covers the distance between MSL and the transition piece (TP). Although the real water depth at the SE Nantucket site is 74.7 m, the design water depth in this study was assumed to be 20 m to match with the dimension of the OC3 monopile. This assumption is common in literature as this study is specifically focused on the effects of wind loading and its directionality on the fatigue analyses [11].

Table 2. Main characteristics of the NREL 5 MW WT and OC3 monopile support structure

Item	Value
Wind regime	IEC Class 1B
Rotor diameter (m)	126
Hub diameter (m)	3
Hub height (m)	90
Cut-in wind speed (m/s)	3
Rated Speed (m/s)	11.4
Cut-out wind speed (m/s)	25
Rated rotor speed (rpm)	12.1
RNA mass (Kg)	350,000
Tower mass (Kg)	347,500
Transition piece height (m)	10
Monopile embedment depth (m)	30
Monopile diameter (m)	6
Monopile thickness (mm)	60

3.2. Generating wind field

In order to design the OWT support structures for fatigue limit state in the normal operational condition, a full range of inflow wind speed (i.e., mean wind speed between cut-in and cut-out wind speeds in which the wind turbine generates energy) should be considered. The IEC standard recommends the minimum intervals of 2 m/s to cover this wind speed range. Therefore, 11 wind fields with mean wind speed of 4, 6, 8, …, 22, 24 m/s were generated for each fatigue analysis. The TurbSim program is used to generate full three-dimensional turbulent wind fields using turbulence spectral parameters estimated based on Kaimal turbulence model [12, 13]. Similar to the approach used to generate the irregular wave signals, eleven different random representations were used to simulate the turbulent wind fields.

3.3. Time domain analyses

Fully coupled aero-hydro-elastic time domain simulations were conducted using the OpenFAST platform [14]. At least six 10-minute or one 1-hour time-history simulations are required for each wind speed bin according to the IEC standard. For this study, the length of all time-domain simulations was 3630 seconds, where the first 30 sec of each simulation was discarded to alleviate the potential impact of the transient state of wind turbine operation on the results of the fatigue analyses. The time-histories of reaction forces and bending moments were obtained at mudline level of the monopile support structure which is considered to carry the maximum bending moments caused by the wind and hydrodynamic loadings. Eight locations around the perimeter of the monopile at the mudline level were considered as the critical spots for the fatigue assessment. These critical spots were evenly distributed over the perimeter of the monopile (i.e., at interval of 45^0), and were located along the main eight wind directions to facilitate the study of the wind directionality effects on the fatigue life of monopiles. The

time-histories of normal stress at the critical locations were calculated based on the estimated reaction forces and bending moments; then, these stress time-histories were used to predict the fatigue damage of the monopile.

3.4. Rainflow cycle counting

The rainflow (RF) cycle counting method was adopted to estimate the total number of stress cycles corresponding to stress range bins, and to create stress range distribution through rainflow matrices [15]. The 1-hour stress time-histories at critical locations were used to create the rainflow matrixes and calculate the number of cycles of different stress cycle ranges for each wind speed bin at each location. Considering the design life of 20 years for the OWT support structures, the total number of stress cycles, that a critical location of a support structure would experience during its lifetime, can be estimated by extrapolating the results from 1-hour simulations to the lifetime of 20 years. Figure 4 presents an example of rainflow matrix which has been extracted from a 1-hour stress time-history at a critical spot of the monopile for the mean wind speed of 12 m/s (i.e., wind speed bin of 11 to 13 m/s).

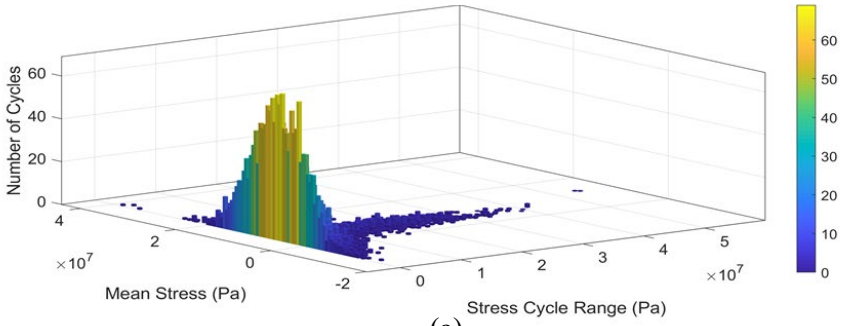

(a)

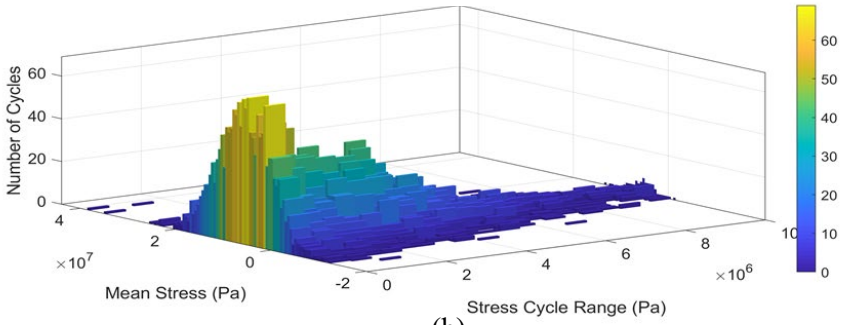

(b)

Figure 4. Rainflow matrix histogram for an hour stress time-history of a critical spot at mudline level of monopile: (a) number of stress cycles for full stress ranges, (b) number of stress cycles for stress ranges up to 10 MPa

4. Fatigue damage assessment

4.1. Characteristic fatigue damage

The most common assumption for the fatigue analysis is that the fatigue damage accumulates linearly (i.e., the damage from the n^{th} cycle is not dependent on any of the previous cycles) [16]. This assumption is known as the Palmgren-Miner's rule which can be presented by the following equation:

$$D_C = \sum_{i=1}^{k} \frac{n_i}{N_i} \leq 1 \tag{2}$$

where D_C is characteristic cumulative fatigue damage, k is number of stress blocks, n_i is number of stress cycles in the stress block i, and N_i is number of stress cycles to failure at constant stress range of $\Delta\sigma_i$. The S-N curves provided in the DNVGL-RP-C203 recommended practice were used to obtain the number of stress cycles to failure and evaluate the fatigue damage [17]. Two proposed categories of the S-N curves in the DNVGL recommended practice were used to estimate the fatigue damage: B1 category for the base material and D category for the weldments. Since the critical spots of the monopile for fatigue damage are located at the mudline level, both categories of the S-N curves were considered in seawater with cathodic protection as well as free corrosion condition to monitor the corrosion fatigue effect [18].

4.2. Effect of mean stress

When the base material is not significantly impacted by residual stresses due to welding or cold forming, the stress range obtained from the rainflow method can be reduced if a part of the stress cycle is in compression according to [17]. The reduction factor is calculated by the following equation:

$$f_m = \frac{\sigma_t + 0.6|\sigma_c|}{\sigma_t + |\sigma_c|} \tag{3}$$

where σ_t is maximum tension stress where tension is defined as positive and σ_c is maximum compression stress where compression is defined as negative. Similarly, when the welded structural details have low residual stresses (e.g., due to post weld heat treatment), the following reduction factor can be used for the weldments:

$$f_m = \frac{\sigma_t + 0.8|\sigma_c|}{\sigma_t + |\sigma_c|} \tag{4}$$

The permission to reduce the stress range for compression stress is due to fact that the compressive stress help close the existing cracks, whereas the tensile stress facilitates the crack opening mechanism and therefore increases the crack growth rate. In this study, the stress reduction factors were applied for both base material and welded components with compressive stress.

4.3. Design fatigue factor

The estimated characteristic fatigue damage is multiplied by design fatigue factor (DFF) to represent the design fatigue damage:

$$D_D = DFF \times D_C \tag{5}$$

The design fatigue factor varies based on: (i) location of critical spots on support structure (i.e., whether fatigue damage is estimated for a critical spot in the atmospheric zone, or in the splash zone, or in the submerged zone); and (ii) possibility and frequency of future inspections. In general, the more difficult to access the critical spots and the less frequency of the planned inspections of the critical spots, the higher the design fatigue factor should be. Since in this study the critical spots are considered at the mudline level, the design fatigue factor is assumed to be 3.0 according to [19].

5. Discussion of results

The location and extent of fatigue damage both change when accounting for the effect of wind directionality. The estimated design fatigue damages for base material of the monopile support structure at the mudline level are illustrated in Figure 5 for both cathodic protection and free corrosion conditions. The same fatigue damages for the weldments are provided in Figure 6. It is observed that by using a constant wind distribution for all directions, the first and second critical location of the fatigue damage

in all cases is on the southwest and west sides of the monopile, respectively. The first and second critical locations shift to the west and northwest sides of the monopile when distinct probability distributions are used for the wind speed in each direction.

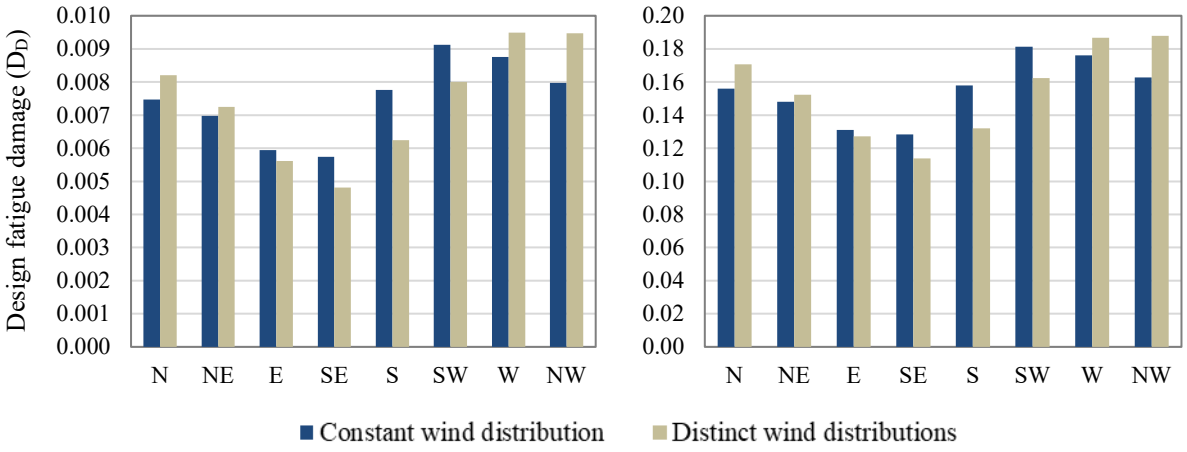

(a) With cathodic protection (b) Free corrosion

Figure 5. Design fatigue damage values for base material at mudline level of monopile

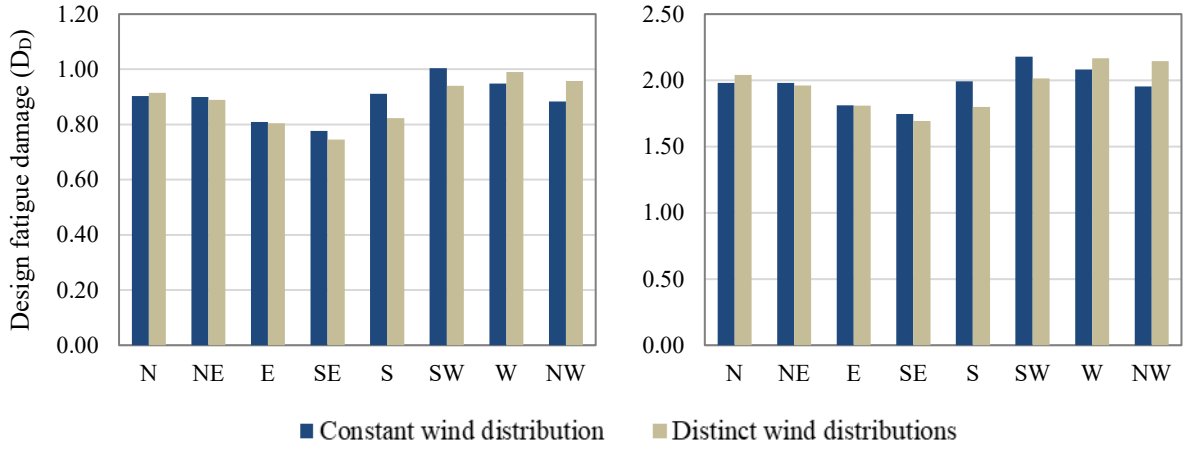

(a) With cathodic protection (b) Free corrosion

Figure 6. Design fatigue damage values for weldments at mudline level of monopile

Discrepancies in the estimated fatigue damage vary for different critical locations. These discrepancies become as high as 22 percent in the south and northwest sides of the monopile while they are the minimum in the east and northeast sides. The discrepancies are generally higher for fatigue damage in base material comparing to the fatigue damage in the weldments.

The other key finding is that despite the case of common practice for multi-directional wind analysis in which the location of the critical spot can be determined with the dominant direction of the wind flow, locating the critical spot is not as intuitive when the effect of multi directionality is taken into consideration. The dominant wind direction in the SE Nantucket site is the southwest direction as reflected in Figure 2 and Table 1. Hence, the critical spot location should be on the southwest side of the monopile due to the fact that more frequent wind flows from southwest direction causes higher compression stresses on northeast side and higher tension stresses on southwest side which latter is more

critical for fatigue design as the stress reduction factor cannot be applied for tensile stress. This is consistent with what is observed in all the cases illustrated in Figure 5 and Figure 6. However, when considering the wind directionality effect, the west and northwest sides of the monopile are located as the critical spot which are not correlated with the dominant wind direction at the wind site.

It is worth mentioning that precise prediction of location of the fatigue damage is of a high importance considering the large diameter of the super large monopiles (i.e., diameter of higher than 10 m) which are currently designed and deployed, and also considering the difficulty of the instrumentation and inspection of the support structures at the mudline.

6. Conclusions

Taking the wind directionality into account has a significant effect on the estimation of the extent of fatigue damage, as well as predicting the critical locations of fatigue damage in monopile support structures. The extent of this effect alters through different fatigue scenarios such as fatigue in base material or weldments, or fatigue damage developing in the corrosive environment. The difference in estimated fatigue damage when the effect of the wind directionality is taken into consideration can be as high as 22 percent comparing to the case that this effect is not considered in the fatigue assessment. Future work will account for higher resolution of the wind directions as well as considering the other types of support structures and more case study wind sites to explore the effect of wind directionality on the fatigue life of the OWT support structures more deeply.

Acknowledgments

This study was supported in part by the Bureau of Ocean and Energy Management of the U.S. Department of Interior (DOI), and the Massachusetts Clean Energy Center. The opinions, findings, and conclusions expressed in this paper are those of the authors and do not necessarily represent the views of the sponsors and organizations involved in this project.

References

[1] EWEA 2013 Energy and the EU budget 2014-20 http://www.ewea.org/fileadmin/files/library/publications/reports/Energy_and_the_EU_budget_2014-2020.pdf

[2] Yeter B, Garbatov Y and Soares C G 2015 Fatigue damage assessment of fixed offshore wind turbine tripod support structures *Engineering Structures* **101** pp 518-528

[3] Musial W and Ram B 2010 Large-scale offshore wind power in the United States – assessment of opportunities and barriers Technical Report NREL/TP-500-40745 NREL Golden, CO, USA

[4] Damiani R, Dykes K and Scott G 2016 A comparison study of offshore wind support structures with monopiles and jackets for U.S. waters *Journal of Physics: Conference Series* **753** (TORQUE 2016) 092003

[5] IEC 61400-3-1 2019 Wind energy generation systems - part 3-1: design requirements for fixed offshore wind turbines International Electrotechnical Commission 309 pp

[6] IEC 61400-1 2019 Wind energy generation systems - part 1: design requirements International Electrotechnical Commission 168 pp

[7] Stewart G M, Robertson A, Jonkman J and Lackner M A 2016 The creation of a comprehensive metocean data set for offshore wind turbine simulations *Wind Energy* **19** issue 6 pp 1151-59

[8] Dong W, Moan T and Gao Z 2012 Fatigue reliability analysis of the jacket support structure for offshore wind turbine considering the effect of corrosion and inspection *Reliability Engineering and System Safety* **106** pp 11-27

[9] Jonkman J, Butterfield S, Musial W and Scott G 2009 Definition of a 5-MW reference wind turbine for offshore system development, Technical Report, NREL/TP-500-38060

[10] Jonkman J and Musial W 2010 Offshore code comparison collaboration (OC3) for IEA task 23 offshore wind technology and development Technical Report NREL/TP-5000-48191

[11] Hafele J, Hubler C, Gebhardt C G and Rolfes R 2018 A comprehensive fatigue load set reduction for offshore wind turbines with jacket sucstructures *Renewable Energy* **118** pp 99-112
[12] Jonkman B J and Kilcher L 2012 TurbSim's user guide: version 1.06.00 Technical Report National Renewable Energy Laboratory Golden, CO, USA
[13] Kaimal J C, Wyngaard J C, Izumi Y and Cote O R 1972 Spectral characteristics of surface-layer turbulence *Q.J.R. Meteorol. Soc.* **98** pp 563-98
[14] OpenFAST 2019 OpenFAST documentation release 1.0 National Renewable Energy Laboratory Golden, CO, USA
[15] ASTM E1049–85 1985 Standard practices for cycle counting in fatigue analysis ASTM International West Conshohocken, PA, USA
[16] Miner M A 1945 Cumulative damage in fatigue *Journal of Applied Mechanics – Trans ASME* **12** A159–64
[17] DNVGL-RP-C203 2019 Fatigue design of offshore steel structures Det Norske Veritas Germanischer Lloyd Recommended Practice 285 pp
[18] Adedipe O, Brennan F and Kolios A 2016 Review of corrosion fatigue in offshore structures: present status and challenges in offshore wind sector *Renewable and Sustainable Energy Reviews* **61** pp 141-54
[19] DNVGL-ST-0126 2016 Support structures for wind turbines Det Norske Veritas Germanischer Lloyd Standard 182 pp